Materials and Design 111 (2016) 344–352

Contents lists available at ScienceDirect

Materials and Design

journal homepage: www.elsevier.com/locate/matdes

# Microstructural evolution of an aged Ni-based superalloy under two-stage hot compression with different strain rates

Kuo-Kuo Li [a,b], Ming-Song Chen [a,b], Y.C. Lin [a,b,c,*], Wu-Quan Yuan [a,b]

[a] *School of Mechanical and Electrical Engineering, Central South University, Changsha 410083, China*
[b] *State Key Laboratory of High Performance Complex Manufacturing, Changsha 410083, China*
[c] *Light Alloy Research Institute of Central South University, Changsha 410083, China*

## HIGHLIGHTS

- Effects of stepped strain rates on the microstructural evolution are significant.
- The appropriate stepped strain rates can obviously promote DRX behaviors.
- DDRX is the primary nucleation mechanism under constant and stepped strain rates.

## GRAPHICAL ABSTRACT

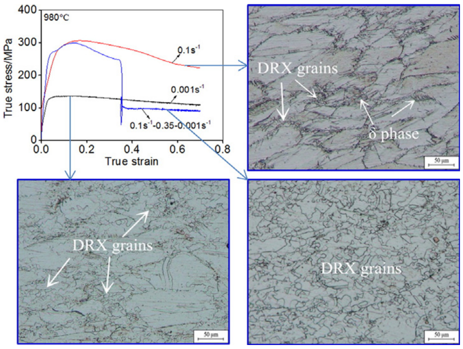

## ARTICLE INFO

*Article history:*
Received 15 August 2016
Received in revised form 31 August 2016
Accepted 3 September 2016
Available online 06 September 2016

*Keywords:*
Hot deformation
Alloy
Dynamic recrystallization
Microstructural evolution

## ABSTRACT

The microstructural evolution of an aged Ni-based superalloy under two-stage hot compressive deformation with different strain rates is investigated. In terms of strain rate, the hot compressive tests include two types: constant and stepped strain rates. For the first type, the strain rate remains constant during the whole hot compression, while for the second type, the hot compression process consists of two stages: I and II. Moreover, the strain rate of stage I (0.01, 0.1, and 1 $s^{-1}$) is larger than that of stage II (0.001 $s^{-1}$). It is found that the strain rate and strain of stage I greatly affect the microstructural evolution for the hot compressive deformation with stepped strain rates. In the tested strain rate and strain, both the dissolution rate of δ phase and the dynamic recrystallization (DRX) volume fraction increase with the decrease of strain rate or the increase of strain in stage I. Compared with the constant strain rate hot deformation, the stepped strain rates can obviously promote DRX behaviors and the dissolution of δ phase if the appropriate strain rate and strain of stage I are chosen. These findings can be directly applied in the practical industrial production of superalloy components.

## 1. Introduction

Generally, metals or alloys experience the complex deformation during hot forming [1,2]. The complex microstructural evolution induced by the work hardening (WH), dynamic recovery (DRV) and dynamic recrystallization (DRX) [3,4,5] usually occurs during the hot

---

[*] Corresponding author at: School of Mechanical and Electrical Engineering, Central South University, Changsha 410083, China.
*E-mail addresses:* yclin@csu.edu.cn, linyongcheng@163.com (Y.C. Lin).

http://dx.doi.org/10.1016/j.matdes.2016.09.007
0264-1275/

deformation of metals or alloys [6,7]. The final microstructures mainly depend on the hot deformation parameters including strain, strain rate and deformation temperature [8,9]. Therefore, it is vital to investigate the effects of hot deformation parameters on the microstructural evolution of materials.

Up to now, some investigations have been done on the microstructural evolution of various metals and alloys, such as AISI 410 martensitic stainless [10], armor steel [11], 35CrMo steel [12], 720Li superalloy [13], Cr-Ni-Mo alloyed steel [14], Mg-9.3Li-1.79Al-1.61Zn alloy [15], 1460 Al-Li alloy [16], Ti-5Al-5Mo-5V-1Cr-1Fe alloy [17], and Al-6Mg-0.4Mn-0.25Sc-0.1Zr alloy [18]. In these researches, the effects of deformation parameters on the microstructural evolution were mainly discussed. For most materials, the high deformation temperature, low strain rate and large strain can accelerate the nucleation and growth of DRX grains. In addition, the effects of chemical component [19] and initial grain size [20] on the microstructural evolution were also investigated.

Ni-based superalloys are widely applied in modern aero engines and gas turbines due to excellent mechanical properties. Some investigations have been carried out on their hot deformation behaviors and microstructural evolution. The effects of deformation temperature, strain rate and strain on the flow stress were studied, and the flow stress constitutive equations of Ni-based superalloys were developed by Liu et al. [21], Etaati et al. [22], Yu et al. [23], Lin et al. [24], Zhang et al. [25], Yang et al. [26], Yang et al. [27], Xu et al. [28], Yao et al. [29], Wang et al. [30], Azarbarmas et al. [31], and Chen et al. [32]. Meanwhile, the effects of the initial content of δ phase ($Ni_3Nb$) on the flow stress were investigated by Lin et al. [33], and an accurate constitutive model to describe the effects of initial δ phase and deformation parameters on hot deformation of GH4169 superalloy was established. Chen et al. [34], Wen et al. [35], and Qin et al. [36] developed the processing maps of Ni-based superalloys. Wen et al. [37] and He et al. [38] investigated the effects of the initial content of δ phase on the processing map of an aged nickel-based superalloy. Additionally, the plastic deformation mechanisms of typical Ni-based superalloys were studied [39,40,41], and some DRX kinetics models of Ni-based superalloys were developed by Chen et al. [42], Reyes et al. [43], and Tancret et al. [44].

Although some investigations have been carried out, the microstructural evolution of aged Ni-based superalloys under inconstant strain rate is still unclear. In this study, the microstructural evolution of an aged Ni-based superalloy under two-stage hot deformation with different strain rates (Named “stepped strain rates”) is investigated by hot compressive tests, optical microscope (OM) and electron backscatter diffraction (EBSD) technology. The effects of stepped strain rates on the evolution of δ phase and grain are discussed.

## 2. Material and experiments

The experimental material is a typical Ni-based superalloy with the composition (wt.%) of 52.82Ni-18.96Cr-5.23Nb-3.01Mo-1.00Ti-0.59Al-0.01Co-0.03C-(bal.) Fe. Cylindrical specimens ($\phi$ 10mm × 12mm) were machined. The heat treatment processing consists of two steps for all specimens, i.e., the specimens were firstly solution treated at 1040 °C for 45 min, then aged at 900 °C for 12 h. Each step was followed by water quenching. The initial optical microstructure of specimens after heat treatment is shown in Fig. 1. As illustrated in Fig. 1, some annealing twins and equiaxed grains can be observed, and large quantities of δ phases ($Ni_3Nb$) appear around grain boundaries while only a few precipitate inside grains. The content of δ phase can be counted as 12.75% using the image software.

The hot compressive tests were done on a Gleeble 3500 thermo-mechanical simulator. The detail schemes are shown in Table 1. The deformation temperature and total true strain for all cases are 980 °C and 0.7, respectively. In terms of strain rate, the hot compressive tests can be divided into two types: constant strain rate and stepped strain rate. For the first type, the strain rate remains constant during the whole hot compression. While for the second type, the hot compression process consists of two stages: I and II. The strain rate of stage I (0.01, 0.1, and 1 $s^{-1}$) is larger than that of stage II (0.001 $s^{-1}$). Taking the case 0.1 $s^{-1}$–0.10–0.001 $s^{-1}$ as an example, the strain rate is 0.1 $s^{-1}$ in stage I, and drops to 0.001 $s^{-1}$ after the true strain is larger than 0.1 (the stage II). Additionally, the case 0.001 $s^{-1}$indicates that the hot compressive test was carried out at the constant strain rate of 0.001 $s^{-1}$. For the both type tests, the specimens were directly heated to deformation temperature at a rate of 10 °C/s, and held for 5 min to minimize the thermal gradient before deformation. After deformation, the specimens were immediately quenched by water.

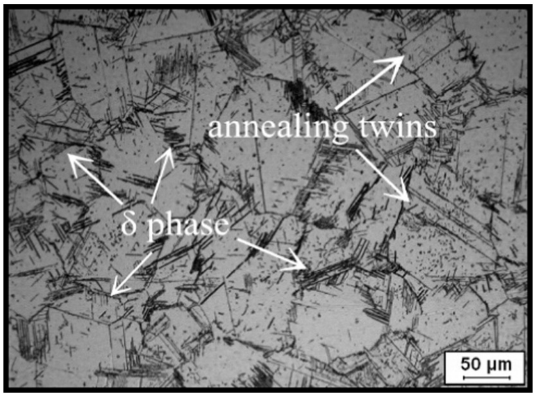

**Fig. 1.** Initial optical microstructure of the specimens after heat treatment.

Optical microscope (OM) and electron backscatter diffraction (EBSD) technology were used to observe the microstructures in the center parts of the section plane. For OM observation, the quenched specimens were split along the longitudinal compression axis. Then, the sections were polished and etched in the solutions of $CuCl_2$ (1 g) + HCl (20 ml) + $CH_3CH_2OH$ (20 ml). For EBSD observation, the foils sliced from the specimens were grinded to 70–80 μm thick. Disks with a diameter of 3 mm were machined from these foils, and then twin-jet electro polished using the corrosive solution of $HClO_4$ and $CH_3CH_3OH$ (1:9 in volume).

## 3. Results and discussion

### 3.1. Analysis of true stress-strain curves

Fig. 2 shows the typical true stress–strain curves obtained from hot compressive tests. In this paper, the hot deformation behaviors under constant strain rate are mainly applied as references. So, the true stress-strain curves under constant strain rate are firstly discussed. As illustrated in Fig. 2a, the stress increases with the increased strain rate. This is mainly because the critical shear stress of dislocation motion increases with the increased strain rate [45]. For each case, the stress firstly increases, then decreases with the increase of strain. The strain for peak flow stress, called peak strain ($\varepsilon_p$), increases with the increase of strain rate. For the aged Ni-based superalloy, the flow stress mainly depends on the average dislocation density, and the morphology and content of δ phases at a given deformation temperature and strain rate. Therefore, the change of flow stress is the reflection of the microstructural evolution of the studied superalloy [1,4,46]. The DRX behavior, the dissolution and deformation of δ phases will lead to the decrease of flow stress. It can be concluded that the rate of DRX and dissolution of δ phases decreases with the increase of strain rate. Fig. 2b shows the typical true stress-strain curves under stepped strain rate (different strain rate in stage I). From Fig. 2b, it can be found that the flow stress suddenly decreases when the strain rate drops to 0.001 $s^{-1}$from large values (0.01, 0.1 and 1 $s^{-1}$). Moreover, the flow stresses in stage II of the cases 1 $s^{-1}$–0.22–0.001 $s^{-1}$, 0.1 $s^{-1}$–0.22–0.001 $s^{-1}$ and 0.01 $s^{-1}$–0.22–0.001 $s^{-1}$are close to that of the case 0.001 $s^{-1}$. The